Initial Gluon Multiplicity in Heavy-Ion Collisions

Alex Krasnitz
UCEH, Universidade do Algarve, Campus de Gambelas, P-8000 Faro, Portugal

Raju Venugopalan
Physics Department, Brookhaven National Laboratory, Upton, New York 11973
(Received 14 July 2000)

The initial gluon multiplicity per unit area per unit rapidity, $dN/L^2/d\eta$, in high energy nuclear collisions, is equal to $f_N(g^2\mu L)\,(g^2\mu)^2/g^2$, with μ^2 proportional to the gluon density per unit area of the colliding nuclei. For an SU(2) gauge theory, we compute $f_N(g^2\mu L) = 0.14 \pm 0.01$ for a wide range in $g^2\mu L$. Extrapolating to SU(3), we predict $dN/L^2/d\eta$ for values of $g^2\mu L$ relevant to the Relativistic Heavy Ion Collider and the Large Hadron Collider. We compute the initial gluon transverse momentum distribution, $dN/L^2/d^2k_\perp$, and show it to be well behaved at low $k_\perp$.

DOI: 10.1103/PhysRevLett.86.1717 PACS numbers: 24.85.+p, 12.38.Mh, 25.75.–q

A topic of considerable current interest is the possibility of forming an equilibrated plasma of quarks and gluons, a quark-gluon plasma (QGP), in very high energy nuclear collisions [1]. Of equal interest is the information that high energy heavy ion collisions provide about the possible saturation of parton distributions in the nuclear wave functions *before* the collision. This saturated state of matter is called a color glass condensate [2] and it is characterized by a bulk momentum scale Q_s. If $Q_s \gg \Lambda_{\rm QCD}$, the properties of this condensate, albeit nonperturbative, can be studied in weak coupling. Partons composing this condensate are freed in the nuclear collision—their subsequent interactions may lead to the formation of the QGP.

The above statements may be quantified in a classical effective field theory approach (EFT) to high energy scattering [3]. The EFT is classical because, at central rapidities, where $x \ll 1$ and $p_\perp \gg \Lambda_{\rm QCD}$, $(x \sim p_\perp/\sqrt{s})$, parton distributions grow rapidly with decreasing x giving rise to large occupation numbers. Briefly, the EFT separates partons in a hadron (or nucleus) into static, high x valence and hard glue sources, and "wee" small x fields. For a large nucleus in the infinite momentum frame, the hard sources with color charge density ρ are randomly distributed in the transverse plane with the distribution

$$P([\rho]) = \exp\left(-\frac{1}{2g^4\mu^2}\int d^2x_\perp \rho^2(x_\perp)\right). \qquad (1)$$

The average squared color charge per unit area is determined by the parameter μ^2, which is the only dimensional parameter in the EFT apart from the linear size L of the nucleus. Parton distributions, correlation functions of the wee gauge fields, are computed by averaging over gauge fields with the weight $P([\rho])$.

Quantum corrections to the EFT are implemented using Wilson renormalization group techniques [4]. The scale $g^2\mu$ grows with decreasing x, and can be estimated from the *nucleon* quark and gluon distributions at $x \ll 1$ [5]. This saturation scale, a function determined self-consistently for the typical x and Q^2 of interest, is roughly related to the scale Q_s mentioned previously through the relation $Q_s \sim 6g^2\mu/4\pi$ [6]. Assuming $g = 2$, the physically relevant values of $g^2\mu$ (Q_s) for RHIC and LHC energies are $\sim$2 ($\sim$1) GeV and $\sim$4 ($\sim$2) GeV, respectively.

The problem of initial conditions [7] for nuclear scattering can be formulated in the classical EFT [8] in the gauge $A^\tau = 0$. Matching the Yang-Mills equations $D_\mu F^{\mu\nu} = J^\nu$ in the four light cone regions, along the light cone, one obtains for the gauge fields in the forward light cone, at proper time $\tau = 0$, the relations $A^i = A_1^i + A_2^i$ and $A^\pm = \pm igx^\pm[A_1^i, A_2^i]/2$. Here $J^\nu = \Sigma_{1,2}\delta^{\nu,\pm}\delta(x^\mp)\rho^{1,2}(x_\perp)$ are random light cone sources corresponding to the valence or hard glue sources in the two nuclei. The transverse pure gauge fields $A_{1,2}^i(\rho^\pm)$, with $i = 1, 2$, are solutions of the Yang-Mills equations for each of the two nuclei before the collision. With these initial conditions, the Yang-Mills equations can be solved in the forward light cone to obtain gluon configurations at late proper times. Since the initial conditions depend on the sources $\rho^\pm$, averages over different realizations of the sources specified by the weight in Eq. (1) must be performed.

Perturbative solutions for the number distributions in transverse momentum, per unit rapidity, were obtained in Refs. [8,9]. In the classical EFT, the number distributions have the form

$$n_{k_\perp} \propto \frac{1}{\alpha_S}\left(\frac{\alpha_S\mu}{k_\perp}\right)^4 \ln\left(\frac{k_\perp}{\alpha_S\mu}\right), \qquad (2)$$

for $k_\perp \gg \alpha_S\mu$. The perturbative description thus breaks down at $k_\perp \sim \alpha_S\mu$. For robust predictions of gluon multiplicity distributions, a fully nonperturbative study of the classical EFT is therefore necessary [10].

Briefly, the model is discretized on a lattice in the transverse plane. Boost invariance and periodic boundary conditions are assumed. The lattice Hamiltonian is the Kogut-Susskind Hamilitonian in $(2 + 1)$ dimensions coupled to an adjoint scalar field. The lattice field equations are then solved by computing the Poisson brackets, with initial conditions that are the lattice analogs of the

continuum initial conditions mentioned earlier. Technical details of our simulations can be found in Refs. [10,11]. Our simulations are presently only for an SU(2) gauge theory; the full SU(3) case will be studied later.

Any dimensional quantity P, well defined within the EFT, can be written in terms of the physically relevant parameters $g^2\mu$ and L as $(g^2\mu)^d f_P(g^2\mu L)$, where d is the dimension of P. The nontrivial physical information is therefore contained in the dimensionless function $f_P(g^2\mu L)$. On the lattice, P will generally depend on the lattice spacing a; this dependence can be removed by taking the continuum limit $a \to 0$. For central Au-Au collisions, we obtain $L = 11.6$ fm as the physical linear dimension of our square lattice. Combining this with the previously mentioned physically relevant values of $g^2\mu$, we obtain $g^2\mu L \approx 120$ (240) for RHIC (LHC).

We now report our results for the initial multiplicity of gluons produced at central rapidities [12]. This quantity, while not directly observable, is related to the number of hadrons produced at central rapidities [13]. The initial multiplicity and momentum distribution of gluons also determine the equilibration time, the temperature, and the chemical potential of the QGP [14,15].

To clarify the meaning of the number of quanta in an interacting non-Abelian gauge theory, consider a free-field theory whose Hamiltonian in momentum space has the form

$$H_f = \frac{1}{2}\sum_k [|\pi(k)|^2 + \omega^2(k)|\phi(k)|^2], \qquad (3)$$

where $\phi(k)$ is the kth momentum component of the field, $\pi(k)$ is its conjugate momentum, and $\omega(k)$ is the corresponding eigenfrequency. The average particle number of the kth mode is then

$$N(k) = \omega(k)\langle|\phi(k)|^2\rangle = \sqrt{\langle|\phi(k)|^2|\pi(k)|^2\rangle}. \qquad (4)$$

In our case, the average $\langle\,\rangle$ is over the initial conditions.

The requirement that the particle number in interacting theories reduces to the standard free-field definition in the weak field limit does not alone define it uniquely outside a free theory. We therefore use two different generalizations of the particle number to an interacting theory. Each has the correct free-field limit. Even though the fields in question are strongly interacting at early times, they are weakly interacting at late times. It is only at this stage that it becomes reasonable to define particle number. We verify that the two definitions agree in this weak-coupling regime.

Our first definition of the multiplicity is straightforward. We impose the Coulomb gauge condition in the transverse plane, $\vec{\nabla}_\perp \cdot \vec{A}_\perp = 0$, and substitute the momentum components of the resulting field configuration into Eq. (4). One option now is to assume $\omega(k_\perp)$ to be the standard massless (lattice) dispersion relation and use the middle expression of Eq. (4) to compute $N(k_\perp)$. Alternatively, we can determine $N(k_\perp)$ from the rightmost expression of Eq. (4); the middle expression of Eq. (4) can then be used to obtain $\omega(k_\perp)$. The second option is preferable; it does not require us to assume that the dispersion relation is linear.

Our second definition is based on the behavior of a free-field theory under cooling. Consider a simple relaxation equation for a field in real space,

$$\partial_t\phi(x) = -\partial H/\partial\phi(x), \qquad (5)$$

where t is the cooling time (*not to be confused with real or proper time*) and H is the Hamiltonian. For a free-field theory ($H = H_f$) the relaxation equation has exactly the same form in the momentum space with the solution $\phi(k,t) = \phi(k,0)\exp[-\omega^2(k)t]$. The potential energy of the relaxed free field is $V(t) = (1/2)\sum_k \omega^2(k)\,|\phi(k,t)|^2$. It is then easy to derive the following integral expression for the total particle number of a free-field system:

$$N = \sqrt{\frac{8}{\pi}}\int_0^\infty \frac{dt}{\sqrt{t}}\,V(t). \qquad (6)$$

Equation (5) can be solved numerically for interacting fields. Subsequently, $V(t)$ can be determined, and N can be computed by numerical integration. In a gauge theory, the relaxation equations are gauge covariant, and the relaxed potential $V(t)$ is gauge invariant, entailing gauge invariance of this definition of the particle number. However, unlike the Coulomb gauge computation discussed earlier,

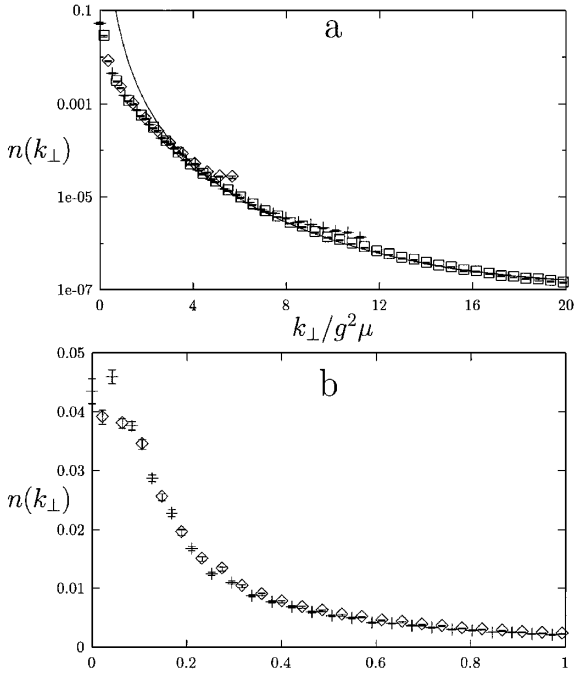

FIG. 1. (a) $n(k_\perp) \equiv dN/L^2/d^2k_\perp$ as a function of the gluon momentum k for $g^2\mu L = 35.35$ and the values 0.138 (squares), 0.276 (plusses), and 0.552 (diamonds) of $g^2\mu a$. The gluon momentum k is in units of $g^2\mu$. The solid line is a fit of the lattice analog of the perturbative expression Eq. (2) to the high-momentum part of the $g^2\mu a = 0.138$ data. (b) $n(k_\perp)$ at soft momenta at $g^2\mu a = 0.29$ for the values 148.5 (plusses) and 297 (diamonds) of $g^2\mu L$.

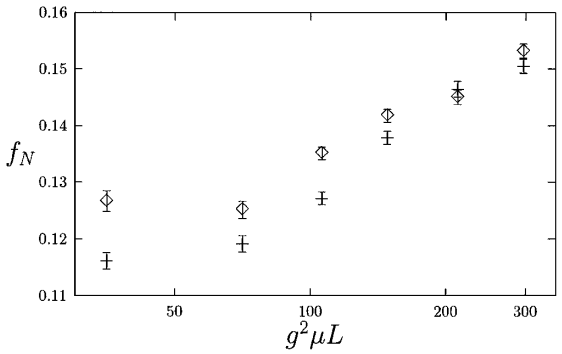

FIG. 2. The function f_N, defined in Eq. (7) as a function of $g^2\mu L$, obtained by the relaxation method (plusses) and by the Coulomb gauge fixing (diamonds). The values of $g^2\mu a$ are 0.276 for $g^2\mu L = 35.35$ and $g^2\mu L = 70.8$; 0.29 for $g^2\mu L = 148.5$ and $g^2\mu L = 297$; and 0.414 for $g^2\mu L = 212$.

this cooling technique presently permits only determination of the total particle number and *not* the number distribution $N(k_\perp)$. Note that both our definitions cease to make sense if the system is far from linearity.

We first present Coulomb gauge results for the number distribution. For $g^2\mu L = 35.35$, in the range of values of $g^2\mu a$ considered here, the system is close to the continuum limit. This is consistent with our earlier analysis of the lattice spacing dependence of a more ultraviolet-sensitive quantity, the energy density [11]. In Fig. 1(a) we plot the gluon number distribution, $n(k_\perp) \equiv dN/L^2/dk_\perp^2 = N(k_\perp)/(2\pi)^2$ versus $k_\perp$ for fixed $g^2\mu L = 35.5$, but for different values of the lattice spacing $g^2\mu a$. Note that for a simple square lattice discretization the Brillouin zone is a square extending from $-\pi/a$ to π/a in each of the principal lattice directions. The momentum $k_\perp$ in Fig. 1 is chosen along a principal direction. The three distributions of Fig. 1(a) agree in the infrared. We therefore conclude that the shape of the distribution at small momenta has converged to the continuum limit. For $k_\perp \gg g^2\mu$, the distribution should be accurately described by the lattice perturbation theory (LPTh) analog of Eq. (2). For large $k_\perp$, on the finest lattice ($g^2\mu a = 0.138$), our numerical result agrees well with LPTh. For the two coarser lattices, even the edge of the Brillouin zone, $k_\perp = \pi/a$, does not quite correspond to the perturbative regime, and the agreement with LPTh is worse. In Fig. 1(b) we plot the gluon distribution in the infrared, at fixed $g^2\mu a$, for different $g^2\mu L$ (148.5 and 297). We notice that these distributions are nearly universal and independent of $g^2\mu L$.

When $k_\perp \leq g^2\mu$, nonperturbative effects qualitatively alter the perturbative number distribution, rendering it finite in the infrared. Unfortunately, since these effects are large, an analytical understanding of the behavior at low $k_\perp$ is lacking.

From our previous discussion, the formula

$$\frac{1}{L^2}\frac{dN}{d\eta} = \frac{1}{g^2} f_N(g^2\mu L)\,(g^2\mu)^2 \tag{7}$$

relates the number of produced gluons per unit area per unit rapidity at zero rapidity to $g^2\mu$. Our results for f_N as a function of $g^2\mu L$, for the smallest values of $g^2\mu a$ feasible, are plotted in Fig. 2. The agreement between the cooling and Coulomb techniques at larger values of $g^2\mu L$ is excellent. It is not as good at the smaller values: in general, the cooling number is more reliable [16]. Figure 2 also demonstrates that the distributions in Fig. 1(b) are not quite universal. This is because f_N is not a constant but has a weak rise with $g^2\mu L$ for larger $g^2\mu L$'s. Table I lists f_N for various $g^2\mu L$. The third row is the Coulomb gauge number after cooling (see Ref. [16]).

In Fig. 3, we plot the dispersion relation $\omega(k_\perp)$ vs $k_\perp$ using the relation Eq. (4). All the dispersion curves rapidly approach the $\omega(k_\perp) = k_\perp$ asymptote characteristic of on-shell partons, while exhibiting a mass gap at zero momentum. For the largest $g^2\mu L$, $m \sim 0.1 g^2\mu$. Since $k_t = 2\pi n/L$, $k_t \sim m$ only for $n \sim 5$. It is thus likely that the gap is not a lattice artifact but is produced by the nonlinear interaction of the gauge fields. We leave a detailed study of the mass gap for a future work.

We can compare our results for the number distribution to the one predicted by Mueller [14]. In terms of Q_s and R, we can rewrite Eq. (7) as

$$\frac{1}{\pi R^2}\frac{dN}{d\eta} = c_N \frac{N_c^2 - 1}{N_c}\frac{1}{4\pi^2\alpha_S} Q_s^2 .$$

Mueller estimates the nonperturbative coefficient c_N to be of order unity. If we take $f_N = 0.14 \pm 0.01$, as is the case for much of the range studied, we find $c_N = 1.29 \pm 0.09$, a number of order unity as predicted by Mueller. However, the transverse momentum distributions, shown in Figs. 1(a) and 1(b), and discussed earlier, differ significantly from Mueller's guess of $\theta(Q_s^2 - k_\perp^2)$.

A large number of models of particle production in nuclear collisions at RHIC and LHC energies can be found in the literature [17]. Naively extrapolating our results to SU(3), we find for Au-Au central collisions at RHIC energies, $dN/d\eta \sim 950$ for $f_N = 0.132 \pm 0.006$

TABLE I. Values of f_N vs $g^2\mu L$, for fixed $g^2\mu a$, plotted in Fig. 2. f_N (res.) is defined in Ref. [16].

$g^2\mu L$	35.36	70.71	106.1	148.5	212.1	297.0
$g^2\mu a$	0.276	0.276	0.207	0.29	0.41	0.29
f_N (cooling)	0.116 ± 0.001	0.119 ± 0.001	0.127 ± 0.001	0.138 ± 0.001	0.146 ± 0.001	0.151 ± 0.001
f_N (Coulomb)	0.127 ± 0.002	0.125 ± 0.002	0.135 ± 0.001	0.142 ± 0.001	0.145 ± 0.001	0.153 ± 0.001
f_N (res.) $\times 10^3$	14 ± 2	7.8 ± 0.2	8.9 ± 0.2	5.6 ± 0.1	7.12 ± 0.08	4.83 ± 0.04

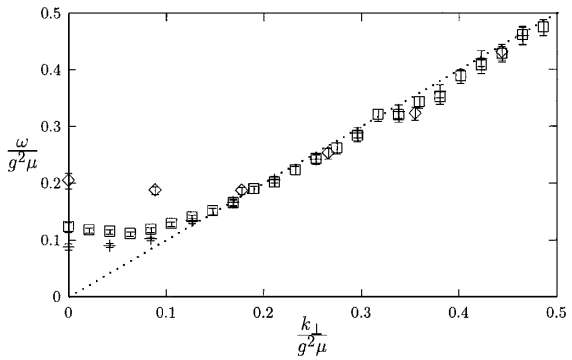

FIG. 3. Gluon dispersion relation $\omega(k_\perp)$ obtained from Eq. (4), for the values 70.8 (diamonds), 148.5 (plusses), and 297 (squares), with the values of $g^2\mu a$ as in Fig. 2.

($g^2\mu L \approx 120$; we take the mean of the 106 and 148 cooling point). Similarly, for LHC energies $f_N = 0.148 \pm 0.002$ ($g^2\mu L \sim 255$, the mean of the 212 and 297 cooling point), one finds $dN/d\eta \sim 4300$. In particular, comparing our predictions with those of perturbative QCD based models [18], we find our numbers to be in rough agreement.

There is considerable uncertainty in the value of Q_s because the gluon densities at the relevant x and Q^2 are ill known. Distinguishing between different models will therefore require, at the very least, testing their predictions for the scaling of multiplicities with centrality, with A and with $\sqrt{s}$. In the EFT, $Q_s \sim A^{1/6}$, hence from Eq. (7) the number per unit rapidity will, up to logarithms of A, be proportional to A. Model predictions for the energy dependence vary significantly, ranging from power law dependences [6,19] of Q_s to $Q_s \propto \exp[\sqrt{\ln(s/s_0)}]$, where s_0 is a constant [20]. Data from RHIC at $\sqrt{s} = 56$ and 130 GeV are already available [21]; the expected data point at $\sqrt{s} = 200$ GeV will make it easier to determine the energy dependence of Q_s.

We thank Larry McLerran and Al Mueller for very useful discussions. R. V.'s research was supported by DOE Contract No. DE-AC02-98CH10886. The authors acknowledge support from the Portuguese FCT, under Grants No. CERN/P/FIS/1203/98 and No. CERN/P/FIS/15196/1999. A. K. thanks the BNL Physics Department for its hospitality.

[1] See, for instance, the *Proceedings of Quark Matter 99* [Nucl. Phys. **A661** (1999)].
[2] Larry McLerran (private communication). For the spin glass analogy, see R. V. Gavai and R. Venugopalan, Phys. Rev. D **54**, 5795 (1996).
[3] L. McLerran and R. Venugopalan, Phys. Rev. D **49**, 2233 (1994); **49**, 3352 (1994); **50**, 2225 (1994).
[4] A. Ayala, J. Jalilian-Marian, L. McLerran, and R. Venugopalan, Phys. Rev. D **52**, 2935 (1995); **53**, 458 (1996); J. Jalilian-Marian, A. Kovner, L. McLerran, and H. Weigert, Phys. Rev. D **55**, 5414 (1997); J. Jalilian-Marian, A. Kovner, A. Leonidov, and H. Weigert, Nucl. Phys. **B504**, 415 (1997); J. Jalilian-Marian, A. Kovner, and H. Weigert, Phys. Rev. D **59**, 014015 (1999); L. McLerran and R. Venugopalan, Phys. Rev. D **59**, 094002 (1999).
[5] M. Gyulassy and L. McLerran, Phys. Rev. C **56**, 2219 (1997).
[6] A. H. Mueller, Nucl. Phys. **B558**, 285 (1999); R. Venugopalan, Acta Phys. Pol. B **30**, 3731 (1999); hep-ph/9907209.
[7] See, for instance, I. Balitsky, Phys. Rev. D **60**, 014020 (1999); Y. V. Kovchegov and A. H. Mueller, Nucl. Phys. **B529**, 451 (1998); S. A. Bass, B. Müller, and W. Poschl, J. Phys. G **25**, L109 (1999).
[8] A. Kovner, L. McLerran, and H. Weigert, Phys. Rev. D **52**, 3809 (1995); **52**, 6231 (1995).
[9] Y. V. Kovchegov and D. H. Rischke, Phys. Rev. C **56**, 1084 (1997); S. G. Matinyan, B. Müller, and D. H. Rischke, Phys. Rev. C **56**, 2191 (1997); **57**, 1927 (1998); Xiao-feng Guo, Phys. Rev. D **59**, 094017 (1999).
[10] A. Krasnitz and R. Venugopalan, hep-ph/9706329; hep-ph/9808332; Nucl. Phys. **B557**, 237 (1999).
[11] A. Krasnitz and R. Venugopalan, Phys. Rev. Lett. **84**, 4309 (2000).
[12] Preliminary results were discussed in A. Krasnitz and R. Venugopalan, hep-ph/0004116.
[13] L. McLerran, hep-ph/9903536.
[14] A. H. Mueller, Nucl. Phys. **B572**, 227 (2000); Phys. Lett. B **475**, 220 (2000).
[15] J. Bjoraker and R. Venugopalan, hep-ph/0008294; R. Baier *et al.,* hep-ph/0009237.
[16] The discrepancy between Coulomb gauge numbers and cooling numbers is likely due to gauge artifacts. The Coulomb gauge number *after* cooling (third row of Table I)—in principle close to zero—added to the gauge invariant cooling number, agrees closely with the Coulomb gauge number *before* cooling.
[17] For a nice compilation, see N. Armesto and C. Pajares, hep-ph/0002163.
[18] K. J. Eskola, K. Kajantie, P. V. Ruuskanen, and K. Tuominen, Nucl. Phys. **B570**, 379 (2000); K. J. Eskola, B. Müller, and X-N. Wang, nucl-th/9608013; K. Geiger, Phys. Rep. **258**, 237 (1995); X-N. Wang, Phys. Rep. **280**, 287 (1997); N. Hammon, H. Stocker, and W. Greiner, Phys. Rev. C **61**, 014901 (2000).
[19] Y. V. Kovchegov, Phys. Rev. D **61**, 074018 (2000).
[20] E. M. Levin and M. G. Ryskin, Phys. Rep. **189**, 267 (1990).
[21] PHOBOS Collaboration, B. B. Back *et al.,* Phys. Rev. Lett. **85**, 3100 (2000).